

# Differentially Expressed Circular RNAs in Stenosed Arteriovenous Fistula Tissues of Uremia Patients

**Lili Lan**

First Affiliated Hospital of Nanchang University

**Yu Liu**

First Affiliated Hospital of Nanchang University

**Menglin Zou**

First Affiliated Hospital of Nanchang University

**Yihang Xie**

Nanchang Hangkong University

**Yiye Zhang**

First Affiliated Hospital of Nanchang University

**Liqing Tian**

First Affiliated Hospital of Nanchang University

**Jun Xiao**

First Affiliated Hospital of Nanchang University

**Liu Yang**

First Affiliated Hospital of Nanchang University

**Li Zhang**

First Affiliated Hospital of Nanchang University

**Yan Yan** (✉ [kiddoc1@163.com](mailto:kiddoc1@163.com))

First Affiliated Hospital of Nanchang University

---

## Research

**Keywords:** arteriovenous fistula, circular RNAs, qRT-PCR, RNA sequencing, uremia

**Posted Date:** September 14th, 2021

**DOI:** <https://doi.org/10.21203/rs.3.rs-864648/v1>

**License:** © ⓘ This work is licensed under a Creative Commons Attribution 4.0 International License.

[Read Full License](#)

---

# Abstract

## Background

Arteriovenous fistula (AVF) is the most common renal replacement therapy for uremic patients. However, stenosis in AVF may lead to AVF failure, hence prevention and effective management of AVF failure is an issue to be addressed. circular RNAs (circRNAs) dysregulation may be pivotal for the development and progression of AVF stenosis.

## Methods

Four stenosed tissues from AVF outflow veins and four normal venous tissues without vascular stenosis were collected for RNA-sequencing (RNA-seq). The circRNAs expression profiles were identified by high-throughput sequencing, and the functions and pathways of differentially expressed (DE) circRNAs were annotated by Gene Ontology (GO) and Kyoto Encyclopedia of Gene Genomes (KEGG) enrichment analyses. Seven DE circRNAs were screened for quantitative real-time polymerase chain reaction (qRT-PCR) validation. circRNA-miRNA interaction network was constructed.

## Results

A total of 17,620 circRNA transcripts were examined by RNA-seq, and 208 DE circRNAs were identified between AG and CG, of which 92 were upregulated and 116 were downregulated. The expression trend in the four selected circRNAs was validated by qRT-PCR, which was consistent with the RNA-seq results. Dysregulated circRNAs may be involved in stenosis by mediating focal adhesion kinase (FAK) pathway.

## Conclusion

Our study revealed abnormal circRNA expression in stenosed tissues of the AVF outflow vein, which was functionally classified. The results indicated that DE circRNAs in the stenosed tissues of AVF and their related FAK pathway have potential to be targets for the prevention and treatment of AVF failure.

## Introduction

Renal replacement therapies (RRTs) are life-saving procedures for uremic patients, and up to 70%~80% of uremic patients are put on hemodialysis (HD) [1]. Arteriovenous fistula (AVF) is strongly recommended by clinical practice guidelines as the preferred method to establish vascular access for most HD patients [2]. The unobstructed vascular access functions essentially in maintaining a high primary patency rate of hemodialysis. However, Kazemzadeh et al. reported that 30% of all AVFs were obstructed and dysfunctional after one year of hemodialysis [3]. AVF failure is an important reason for hospitalization and inadequate hemodialysis, and the prevention and effective management of AVF failure is an urgent issue to be solved. Studies show that venous neointimal hyperplasia (VNH) that can narrow the lumen of the AVF outflow vein, especially near the fistula anastomosis, is considered as the primary contributor in facilitating irreversible AVF stenosis [4, 17]. Excessive proliferation and migration of vascular smooth

muscle cells (VSMC) at the AVF outflow vein is a pivotal factor in the development and progression of vascular neointimal hyperplasia and vascular remodeling [5]. There are very few studies on the underlying mechanisms of AVF stenosis, and therefore exploration of VSMC proliferation and migration may be crucial in prevention and management of AVF failure.

Circular RNAs (circRNAs) are different from traditional RNAs and belong to an endogenous non-coding (nc) RNA family, forming a closed annular structure by back-splicing circularization, which contains neither 5' end caps nor 3' end poly tails [6]. This special structure makes circRNAs unusually stable and resistant to RNase digestion. Recent studies have revealed that circRNAs are widespread in exosomes and cytoplasm of eukaryotic cells [7], and their expressions are tissue-specific [8]. Additionally, they are closely associated with the physiology and pathology of vascular diseases via microRNA (miRNA) sponges that regulate mRNA expressions [9]. Recent studies have revealed that differentially expressed (DE) circRNAs are involved in the development of various vascular diseases by regulating VSMC proliferation and migration. Chen et al. suggested that circWDR77 (WD repeat domain 77) promotes proliferation and migration of high glucose induced VSMC in diabetes mellitus correlated vasculopathy through targeting miR-124/FGF2 (fibroblast growth factor 2) [10]. In addition, the checkpoint with forkhead-associated and ring-finger domains (circ\_CHFR) over-expression regulates human VSMC proliferation and migration by functioning as a miR-214-3p sponge, which is associated with the atherosclerosis (AS) progression [11]. Therefore, circRNAs may have potential in managing various vascular diseases including AVF stenosis.

Hitherto, there had been few studies concerning circRNAs profile and the role of DE circRNAs in VSMC proliferation and migration in stenosed tissue in AVF. Present study utilized bioinformatics to comprehensively analyze the alteration of circRNA expression profile in the stenosed tissues of the AVF outflow vein and normal venous tissue. The study also explored their potential functions in the development of AVF dysfunction for the first time. Seven dysregulated circRNAs from these DE circRNAs were screened, which were verified by quantitative real-time polymerase chain reaction (qRT-PCR). Finally, a putative interaction network of circRNA-miRNA was constructed. Our study aimed to provide fundamental experimental data for exploring the differential expression of circRNAs that may be involved in the development and progression of AVF dysfunction.

## Methods

### Patients and tissue samples

All the vascular tissues were collected from uremic patients in the Department of Nephrology in the First Affiliated Hospital of Nanchang University between February 2017 and March 2017. Four patients were randomly selected from hemodialysis patients with confirmed diagnosis of AVF stenosis and were included in the AVF stenosis group (AG). And four patients were randomly selected from a pool of uremic patients who had undergone primary AVF surgery and were then categorized as the control group (CG).

Written informed consent forms were obtained from the patients. All samples were acquired after approval and authorization by the First Affiliated Hospital of Nanchang University Ethics Committee.

The AG inclusion criteria included: age of AVF > 3 months; the stenosis was in the juxta-anastomotic venous segment; clinical signs of AVF dysfunction: insufficient arterial blood flow of the AVF during dialysis: < 200 ml/min, the ultrasonography documented significant AVF stenosis (defined as more than 50% stenosis in the minimal luminal diameter of the AVF compared to the vessel diameter of the most proximal normal vein) and without obvious thrombosis in the venous wall. Exclusion criteria include: using anticancer drugs, or systemic corticosteroid, immunosuppressive drugs and other anti-inflammatory drug. The uremic patients who were included in CG would not have obvious vascular stenosis or vascular diseases. The vascular tissues from the two groups were acquired from the AVF outflow veins anastomosed to the radial arteries or brachial arteries. Four experimental samples from AG and four control samples from CG were used for high-throughput RNA-sequencing. The clinical characteristics of the patients are summarized in Supplementary Table 1. Vascular tissue samples collected from surgery were immediately placed in cryopreserved tubes with 2 ml RNA, which were quickly transferred into a refrigerator at 4°C for 24 hours. The samples were stored in a refrigerator at -80°C, until RNA isolation.

## **RNA preparation, library establishment and high-throughput sequencing**

Our lab extracted total RNA from vascular tissues using TRIzol reagent (Invitrogen Life Technologies) following the manufacturer's instructions. The quality of total RNA in each sample was evaluated by NanoDrop spectrophotometer (Thermo Scientific). RNA integrity was further analyzed through Bioanalyzer 2100 system (Agilent Technologies). The Ribo-zero Gold rRNA Removal kit (Illumina, San Diego, CA, USA) was employed to remove ribosomal RNAs (rRNAs) from total RNA following the standard. After extracting the rRNA, the remaining RNA was fragmented into 200–300 base pairs (bp) in length using divalent cations under elevated temperature in an Illumina proprietary fragmentation buffer [12]. These fragmentations were transcribed into single-stranded complementary DNA (cDNA) and single-stranded cDNA synthesis was performed for establishing specific RNA libraries leveraging Truseq Stranded Sample Preparation Kit (Illumina) following the standard procedure. Quality control assay for sequencing libraries was carried out by utilizing the Agilent Bioanalyzer 2100 system. Employing the Next-Generation sequencing (NGS), we implemented paired-end sequencing for 300–400 bp length DNA fragments on an Illumina Hiseq platform.

## **circRNAs identification and analysis in both groups**

We acquired raw data from NGS on an Hiseq platform (Illumina). To screen high quality data, 3' adaptors were trimmed and low-quality reads were removed using cutadapt software (<https://cutadapt.readthedocs.io/en/stable/>). The high-quality reads were compared with the human reference genome hg38 using Tophat2(<http://tophat.cbcb.umd.edu/>) and the reference genome data was acquired from the Ensembl database (<http://ensembl.org/>). Anchor reads captured from both ends of

unmapped reads of each sample were mapped to the reference genome. The *find\_circ* software was utilized to identify and screen circRNAs after the results were combined. circRNAs abundances were normalized via obtaining the reads per kilobase per million reads (RPKM).

## Differentially expressed circRNAs between AVF stenosis and control groups

To analyze the transcript expression alternations between AG and CG, we calculated the differentially expressed levels of circRNAs using DESeq (Version 1.18.0). circRNAs with fold change greater than 2 or less than -2 and P value < 0.05 were considered as significant difference in expression. Hierarchical cluster analysis was carried out to distinguish the expression patterns of circRNAs between AG and CG using R software. Same color regions represent cluster grouping information. In addition, the ggplot2 of the ballgown R package was adapted to draw volcanic plot of differential expression transcripts, which identified DE circRNAs with statistical significance (P > 0.05) between two groups.

## Parental gene enrichment of DE circRNAs and functional annotation

To explore potential functions of the DE circRNAs that may be involved in the development of AVF stenosis in uremic patients, Gene Ontology (GO) and Kyoto Encyclopedia of Gene Genome (KEGG) enrichment analyses were performed for corresponding parental genes. GO annotation was divided into three categories: molecular function (MF), biological progress (BP), and cellular components (CC). GO terms were significantly enriched at P value < 0.05. To mainly identify metabolic and signaling pathways of DE circRNAs in the AVF stenosis tissue, we counted the hosting protein-coding genes from which circRNAs were derived on each KEGG pathway.

## Quantitative real-time PCR (qRT-PCR) validation

Seven circRNAs (hsa\_circ\_015036, hsa\_circ\_005718, hsa\_circ\_007293, hsa\_circ\_017814, hsa\_circ\_026394, hsa\_circ\_035577, and hsa\_circ\_019184) were selected to further validate the RNA-sequencing results by employing qRT-PCR assays. Following the manufacturer instructions, reverse transcription reaction was conducted to synthesize single-stranded complementary DNA (cDNA) by RevertAid First Strand cDNA Synthesis Kit (Thermo Fermentas, Beijing, China) using random primers. The cDNA was used as a template to perform qRT-PCR. The qRT-PCR was implemented with 2\*PCR Master Mix (Roche, Switzerland) according to manufacturer's instructions. In brief, the cDNA amplification steps were as follows: 95°C for 10 minutes; 45 cycles at 95°C for 15 seconds, and 60°C for 60 seconds; slowly progress from 60°C to 99°C. The cDNA amplification was in triplicate for each group. The amplification efficiency was assessed via standard curve analysis. H-Actin was utilized as a reference gene, and the relative expression levels of candidate circRNAs between the two groups were calculated using the  $2^{-\Delta\Delta CT}$  method. The primers for qRT-PCR are listed in Supplementary Table 2.

## Target miRNA prediction and co-expression network establishment

A recent study has reported that circRNAs located in the cytoplasm contain complementary miRNA binding sites, which serve as competitive inhibitors for miRNAs. The DE circRNAs interacting with their target miRNAs result in repressing mRNA cleavage and trigger mRNA translation [13]. To further dissect the potential DE circRNA functions in AVF dysfunction development and progression, the miRNA-binding sites of four DE circRNAs (hsa\_circ\_015036, hsa\_circ\_005718, hsa\_circ\_017814, and hsa\_circ\_007293) were predicted via using miRanda software, which were validated by qRT-PCR. A perfect seed matching between miRNA and target circRNA was considered for a MiRanda score of 140 or higher [14]. The interaction network between the four candidate circRNAs and their corresponding target miRNAs was constructed using Cytoscape 3.6.1.

## Statistical analysis

Data analysis was performed by Statistical Program for Social Sciences (SPSS) 22.0 software and the results were denoted by mean  $\pm$  standard deviation. The significant differences of sequencing data between the two groups were assessed via Student's t-test and fold change. The statistical significance threshold was considered as P value  $< 0.05$ .

## Results

### Characteristics of circRNA expression pattern in stenosed AVF tissues

circRNA sequencing to explore the profile was initiated on Illumina Hiseq platform by analyzing four stenosed AVF tissues and four control vascular tissues from the ESRD patients. 17,620 circRNAs were identified, and their distribution characteristics on chromosomes are illustrated in Supplementary Fig. 1A. These circRNAs were transcribed from all human chromosomes including 22 autosomes and 2 gonosomes, most of which were distributed on chromosome 1, chromosome 2, chromosome 4, and chromosome 6. The least distribution is on chromosome Y. Moreover, the top 10 upregulated or downregulated circRNAs were mainly scattered on chromosome 1. Based on the properties of parental genes from which circRNAs are derived, the high-quality circRNAs identified by find\_circ were categorized as annot\_exons, antisense, intergenic, intron\_exon, intronic, and one\_exon. The proportion of annot\_exons was found to be the largest (Supplementary Fig. 1B).

### Identification of differentially expressed circRNAs between AG and CG

The correlation of circRNA expression pattern between samples was tested before the DE circRNA analysis, and we show the correlation coefficients in Fig. 1 (the coefficient is closer to 1, the expression pattern between samples is more similar). Hierarchical cluster analysis was used to display the expression levels of circRNAs in the two group samples. The heatmap exhibited that there was significant difference in circRNA expression in the two groups (Fig. 2). Based on the filter criteria of fold change  $> 2$  or  $< -2$  and P value  $< 0.05$ , we identified 208 DE circRNAs between AG and CG. Among these, 92 DE

circRNAs were significantly over-expressed and 116 circRNAs decreased more than two-fold in AG comparing to CG. Volcano plot authenticated the fold change of circRNAs after log<sub>2</sub> transformations were clearly differentiated, which showed that the distribution was roughly symmetrical in the two groups (Supplementary Fig. 2). Supplementary Table 3 lists the top 10 DE circRNAs that were significantly upregulated or downregulated.

## Functional enrichment analysis of DE circRNA parental genes

We observed that the parental genes of 208 DE circRNAs were assigned to 1,959 GO terms, which included 1,450 GO terms enriched for BP, 269 GO terms enriched for MF, and 240 GO terms enriched for CC. In Fig. 3, we see that there are 6 GO terms assessable with P value < 0.05. The majority of the hosting protein-coding genes of DE circRNAs were significantly enriched in BP such as single-multicellular organism process, anatomical structure development, and multicellular organism development. For MF, there are four parental genes related to alpha-actinin binding (P value < 0.05). Other genes may be associated with metal ion binding and cytoskeletal protein binding though the results were not significant (P value > 0.05). Some genes enriched in CC correlated with voltage-gated calcium channel complex, cell leading edge, and basal lamina. Unfortunately, there was no significant correlation (P value > 0.05).

The top 20 KEGG pathways that significantly enriched are presented in Supplementary Fig. 3, which include focal adhesion (FA), regulation of actin cytoskeleton, vascular smooth muscle contraction, and ErbB signaling pathway. FA was the most significantly enriched pathway, and most of DE circRNAs were involved in the FA also (Transcript count = 11). Results indicated that DE circRNAs may be involved in AVF stenosis development and progression through interference of the motility and metabolism of VSMC from the AVF outflow vein.

## Validation of candidate circRNAs in AVF stenotic tissue

Seven candidate circRNAs (downregulated: hsa\_circ\_015036, hsa\_circ\_005718, hsa\_circ\_017814, hsa\_circ\_019184, upregulated: hsa\_circ\_007293, hsa\_circ\_026394, and hsa\_circ\_035577) were filtered out to validate the reliability of previous RNA-sequencing results, and their expression levels between AG and CG were detected using qRT-PCR. The candidate circRNAs satisfied following conditions: (1) fold change > 2 or < -2; (2) P value < 0.05; (3) the host protein-coding genes of candidate circRNAs were involved in FA signal pathway, which may be highly correlated with AVF dysfunction. Based on qRT-PCR results, the hsa\_circ\_026394 and hsa\_circ\_035577 expression trends in the two groups were consistent with the RNA-sequencing results, but there was no significant statistical difference (P value > 0.05). Moreover, hsa\_circ\_019184 expression abundance in the two samples was too low to be detected. Therefore hsa\_circ\_019184, hsa\_circ\_026394 and hsa\_circ\_035577 were excluded for further study. The hsa\_circ\_007293 expression levels in AG were significantly higher in CG, and hsa\_circ\_015036, hsa\_circ\_005718, and hsa\_circ\_017814 were significantly under-expressed in stenosed AVF tissues

comparing to normal vascular tissues, which mostly followed the circRNA transcript expression trends that detected by RNA-sequencing (Fig. 4).

## Establishing interaction network between target miRNAs and candidate circRNAs

We further predicted miRNA binding sites on four candidate circRNAs (hsa\_circ\_015036, hsa\_circ\_005718, hsa\_circ\_017814, and hsa\_circ\_007293) through miRanda software, which included three downregulated circRNAs and one upregulated circRNA. Based on the criteria of max score  $\geq 140$  and max energy  $\leq -25$  [14], a total of 134 miRNA were paired with four DE circRNAs after discarding the repeated values. For each candidate circRNA, top 10 target miRNAs with the highest degree of correlation were considered (a lower max energy is indicative of a stronger correlation) [14], then we acquired 38 miRNAs after discarding repeating target miRNAs. Figure 5 illustrates the miRNA-circRNA interaction network regarding the four candidate circRNAs.

## Discussion

The stenotic lesions in AVF involve multiple pathological factors. Many studies indicated that neointimal hyperplasia in the vascular lumen of AVF is a pathological event. Others include oxidative stress, inflammation, shear stress, and pre-existent vascular lesions [15–17]. Venous neointimal hyperplasia in AVF with an outflow stenosis is associated with vascular cell activation and migration as well as extracellular matrix remodeling with complicated interactions between adhesion molecules, inflammatory mediators, and growth factor [17]. Recently, with the rapid advancement of RNA-sequencing technology and bioinformatics, circRNAs are increasingly explored. Various studies demonstrated that circRNAs could be employed as new clinical biomarkers of diverse vascular diseases such like atherosclerosis [18], pulmonary arterial hypertension [19], and coronary heart disease [20]. CircRNAs were demonstrated to be enriched in vascular tissues and function importantly in VSMC proliferation and migration [10, 11, 20]. circ-SATB2 over-expression promotes VSMC proliferation and migration, which inhibits their phenotypic differentiation by regulating miR-939 expression in coronary heart disease (CHD) [20]. Several investigations revealed the potential correlations between circRNAs and various vascular diseases, however, the circRNA expression profiles in the stenosis tissue of the AVF outflow vein and their underlying functions were unclear.

In present study, the circRNA expression profile in venous tissue of AVF with an outflow stenosis was identified for the first time through circRNA high-throughput sequencing. To study the mechanism of AVF dysfunction in detail, the circRNA profile was screened to discover their differential expression. 208 DE circRNAs were identified in the vascular tissues of uremic patients with AVF stenosis and patients in the control group. Further DE circRNA investigations may help us understand their functions in AVF stenosis. GO and KEGG pathway analysis were performed in this study, and results revealed that majority of DE circRNAs were associated with FA pathway. The FA structure comprised of the extra cellular matrix (ECM), transmembrane proteins (known as integrins), and intracellular actin microfilament [21, 22]. Many

signaling molecules play a prominent role in the integrin signaling pathway such as focal adhesion kinase (FAK) [23, 24]. Previous studies have shown that FAK belongs to the non-receptor tyrosine kinase family, which may correlate closely with VSMC proliferation and migration in various vascular diseases [25–27]. Li et al. proposed that periostin (a novel ECM protein) promotes VSMC migration by interacting with alphaV-integrins and subsequently activating FAK pathway. This process results in vascular neointima formation in atherosclerosis and restenosis after vascular intervention [26]. Morla et al. suggested that extracellular matrix proteins such as fibronectin (FN) and laminin (LM) regulate VSMC phenotype and proliferation via FAK signaling pathway in pathological states such as restenosis [27]. Therefore, FAK pathway may serve as an indispensable target in future therapies aiming at neointimal proliferation reduction in vascular diseases. Our team selected 7 DE circRNAs that were involved in the FAK pathway for further qRT-PCR validation based on KEGG pathway analysis. Based on the results of high-throughput sequencing and qRT-PCR, the hsa\_circ\_015036 and hsa\_circ\_005718 downregulations in stenosed AVF tissues were most significant. While further studies are required to determine whether DE circRNAs and FAK pathway are important targets in AVF failure prevention and treatment.

## Conclusion

In conclusion, our study was the first to identify circRNAs that expressed abnormally in the stenosed AVF tissues. We functionally classified circRNAs through bioinformatics approaches and validated 4 dysregulated circRNAs mediating the FAK pathway through qRT-PCR. The hsa\_circ\_015036, hsa\_circ\_005718, and hsa\_circ\_017814 expression levels decreased remarkably and hsa\_circ\_007293 expression elevated dramatically. The hsa\_circ\_015036 and hsa\_circ\_005718 downregulations might promote VSMC proliferation and migration of AVF outflow vein by mediating the FAK pathway. This may promote venous neointimal hyperplasia and then exert regulatory functions in AVF stenosis development and progression. The data show that DE circRNAs and related FAK pathway have great potential to be targets of AVF dysfunction prevention and treatment in uremia patients. This is a new insight for further exploration of the DE circRNA roles in AVF stenosis development and progression.

This study acquired the differential expression profile of circRNAs in the stenosed tissue of the AVF outflow vein. 208 DE circRNAs were identified, which may be involved in AVF failure as per GO and KEGG enrichment analyses. According to the RNA-sequencing and qRT-PCR data, we surmise that the abnormal hsa\_circ\_015036 and hsa\_circ\_005718 expressions may enhance VSMC proliferation and migration of the AVF outflow vein via FAK pathway, which may function importantly in AVF failure development and progression. In the future, we would further explore the potential of DE circRNAs as targets along with their pathological effects in AVF failure.

## Declarations

### AUTHOR CONTRIBUTIONS

YY conceived, designed and supervised the study. LL, YL and MZ performed the bioinformatics analyses. YL and YX performed qRT-PCR assay. LL wrote the manuscript. YZ, LT and JX analyzed the data. LY and LZ revised the manuscript. All authors read and approved the final manuscript.

### **Availability of data and materials**

The dataset(s) supporting the conclusions of this article is(are) included within the article (and its additional file(s))

### **Ethics approval and consent to participate**

All samples were acquired after approval and authorization by the Ethics Committee in First Affiliated Hospital of Nanchang University.

### **Consent for publication**

All authors gave consent for the publication.

### **Competing Interests**

The authors have declared that they have no competing interests.

### **Funding**

Not applicable.

### **Acknowledgment**

Not applicable.

## **References**

1. Lok CE, Foley R. Vascular access morbidity and mortality: trends of the last decade. *Clin J Am Soc Nephrol.* 2013;8(7):1213-9.
2. Ravani P, Palmer SC, Oliver MJ, et al. Associations between hemodialysis access type and clinical outcomes: a systematic review. *J Am Soc Nephrol.* 2013;24(3):465-73.
3. Gh K, Mhs M, H R, M D, L H, M N. Primary patency rate of native AV fistula: long term follow up. *Int J Clin Exp Med.* 2012;5(2):173-8.
4. Rothuizen TC, Wong C, Quax PH, van Zonneveld AJ, Rabelink TJ, Rotmans JI. Arteriovenous access failure: more than just intimal hyperplasia? *Nephrol Dial Transplant.* 2013;28(5):1085-92.
5. Guo Q, Huang F, Qing Y, et al. Decreased Jagged1 expression in vascular smooth muscle cells delays endothelial regeneration in arteriovenous graft. *Cardiovasc Res.* 2020;116(13):2142-55.
6. Hentze MW, Preiss T. Circular RNAs: splicing's enigma variations. *EMBO J.* 2013;32(7):923-5.

7. Li Y, Zheng Q, Bao C, et al. Circular RNA is enriched and stable in exosomes: a promising biomarker for cancer diagnosis. *Cell Res.* 2015;25(8):981-4.
8. Maass PG, Glažar P, Memczak S, et al. A map of human circular RNAs in clinically relevant tissues. *J Mol Med (Berl).* 2017;95(11):1179-89.
9. Hansen TB, Jensen TI, Clausen BH, et al. Natural RNA circles function as efficient microRNA sponges. *Nature.* 2013;495(7441):384-8.
10. Chen J, Cui L, Yuan J, Zhang Y, Sang H. Circular RNA WDR77 target FGF-2 to regulate vascular smooth muscle cells proliferation and migration by sponging miR-124. *Biochem Biophys Res Commun.* 2017;494(1-2):126-32.
11. Zhuang JB, Li T, Hu XM, et al. Circ\_CHFR expedites cell growth, migration and inflammation in ox-LDL-treated human vascular smooth muscle cells via the miR-214-3p/Wnt3/ $\beta$ -catenin pathway. *Eur Rev Med Pharmacol Sci.* 2020;24(6):3282-92.
12. Yan Y, Ye W, Chen Q, et al. Differential expression profile of long non-coding RNA in the stenosis tissue of arteriovenous fistula. *Gene.* 2018; 664: 127-38.
13. Li R, Jiang J, Shi H, Qian H, Zhang X, Xu W. CircRNA: a rising star in gastric cancer. *Cell Mol Life Sci.* 2020;77(9):1661-80.
14. Su X, Gao G, Wang S, et al. CircRNA expression profile of bovine placentas in late gestation with aberrant SCNT fetus. *J Clin Lab Anal.* 2019;33(6):e22918.
15. Gjorgjievski N, Dzekova-Vidimliski P, Gerasimovska V, et al. Primary Failure of the Arteriovenous Fistula in Patients with Chronic Kidney Disease Stage 4/5. *Open Access Maced J Med Sci.* 2019;7(11):1782-7.
16. Pushevski V, Dejanov P, Gerasimovska V, et al. Severe Endothelial Damage in Chronic Kidney Disease Patients Prior to Haemodialysis Vascular Access Surgery. *Pril (Makedon Akad Nauk Umet Odd Med Nauki).* 2015;36(3):43-9.
17. Hu H, Patel S, Hanisch JJ, et al. Future research directions to improve fistula maturation and reduce access failure. *Semin Vasc Surg.* 2016;29(4):153-71.
18. Zhuang JB, Li T, Hu XM, et al. Circ\_CHFR expedites cell growth, migration and inflammation in ox-LDL-treated human vascular smooth muscle cells via the miR-214-3p/Wnt3/ $\beta$ -catenin pathway. *Eur Rev Med Pharmacol Sci.* 2020;24(6):3282-92.
19. Zhou S, Jiang H, Li M, et al. Circular RNA hsa\_circ\_0016070 Is Associated with Pulmonary Arterial Hypertension by Promoting PSMC Proliferation. *Mol Ther Nucleic Acids.* 2019;18:275-84.
20. Mao YY, Wang JQ, Guo XX, Bi Y, Wang CX. Circ-SATB2 upregulates STIM1 expression and regulates vascular smooth muscle cell proliferation and differentiation through miR-939. *Biochem Biophys Res Commun.* 2018;505(1):119-25.
21. Burridge K, Fath K, Kelly T, Nuckolls G, Turner C. Focal adhesions: transmembrane junctions between the extracellular matrix and the cytoskeleton. *Annu Rev Cell Biol.* 1988;4:487-525.

22. Owen GR, Meredith DO, ap Gwynn I, Richards RG. Focal adhesion quantification - a new assay of material biocompatibility? Review. *Eur Cell Mater.* 2005; 9:85-96.
23. Shibasaki F, Fukami K, Fukui Y, Takenawa T. Phosphatidylinositol 3-kinase binds to alpha-actinin through the p85 subunit. *Biochem J.* 1994;302 (Pt 2)(Pt 2):551-7.
24. Parsons JT. Focal adhesion kinase: the first ten years. *J Cell Sci.* 2003;116(Pt 8):1409-16.
25. Ilić D, Damsky CH, Yamamoto T. Focal adhesion kinase: at the crossroads of signal transduction. *J Cell Sci.* 1997;110 (Pt 4):401-7.
26. Li G, Jin R, Norris RA, et al. Periostin mediates vascular smooth muscle cell migration through the integrins alphavbeta3 and alphavbeta5 and focal adhesion kinase (FAK) pathway. *Atherosclerosis.* 2010;208(2):358-65.
27. Morla AO, Mogford JE. Control of smooth muscle cell proliferation and phenotype by integrin signaling through focal adhesion kinase. *Biochem Biophys Res Commun.* 2000;272(1):298-302.

## Figures

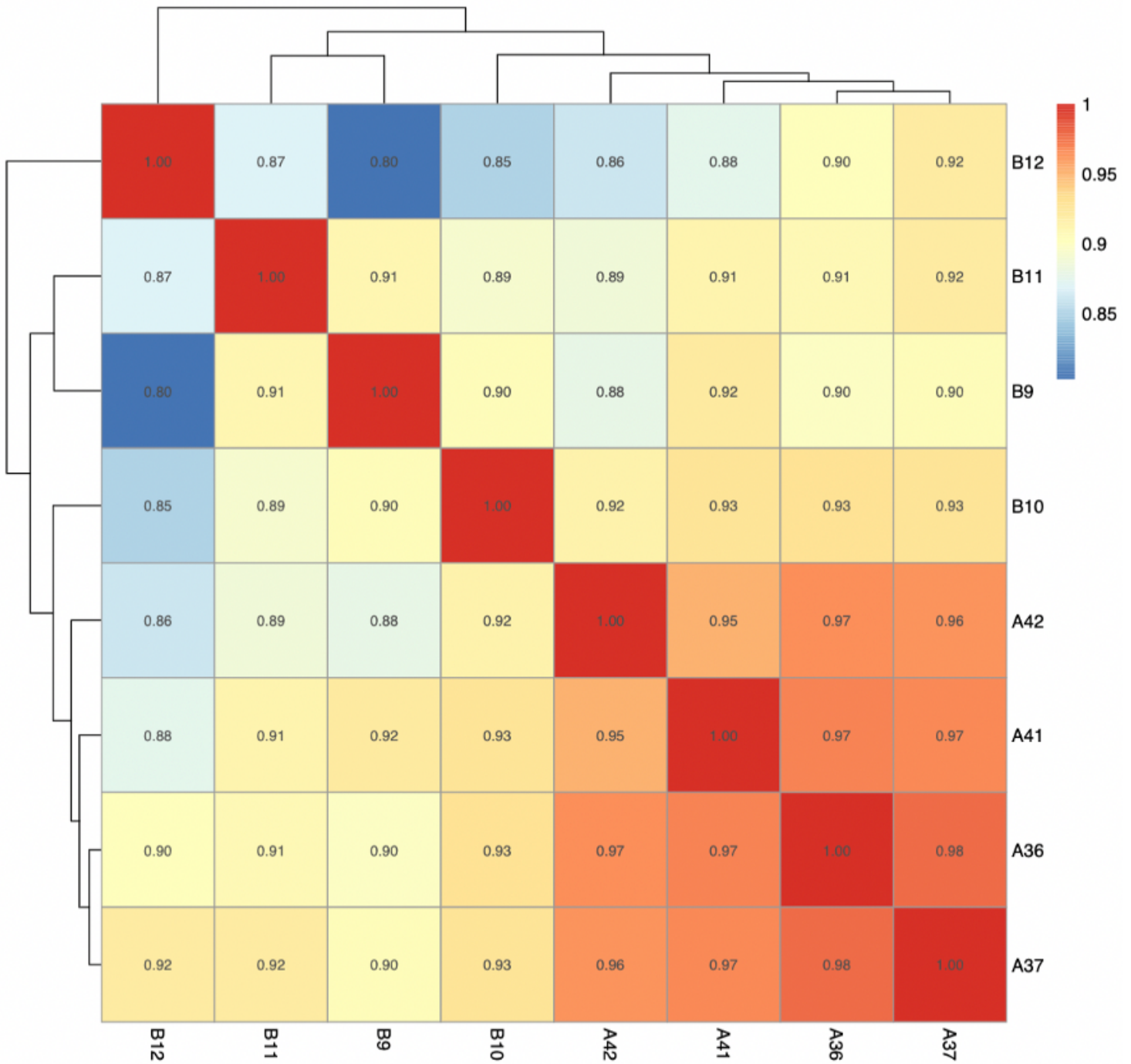


**Figure 1**

Scatter plot of correlation of gene expression pattern between the two groups. The value in the squares represent the coefficient degree between samples: the value is close to 1, the correlation is higher. Red squares: strong correlation; blue squares: low correlation.

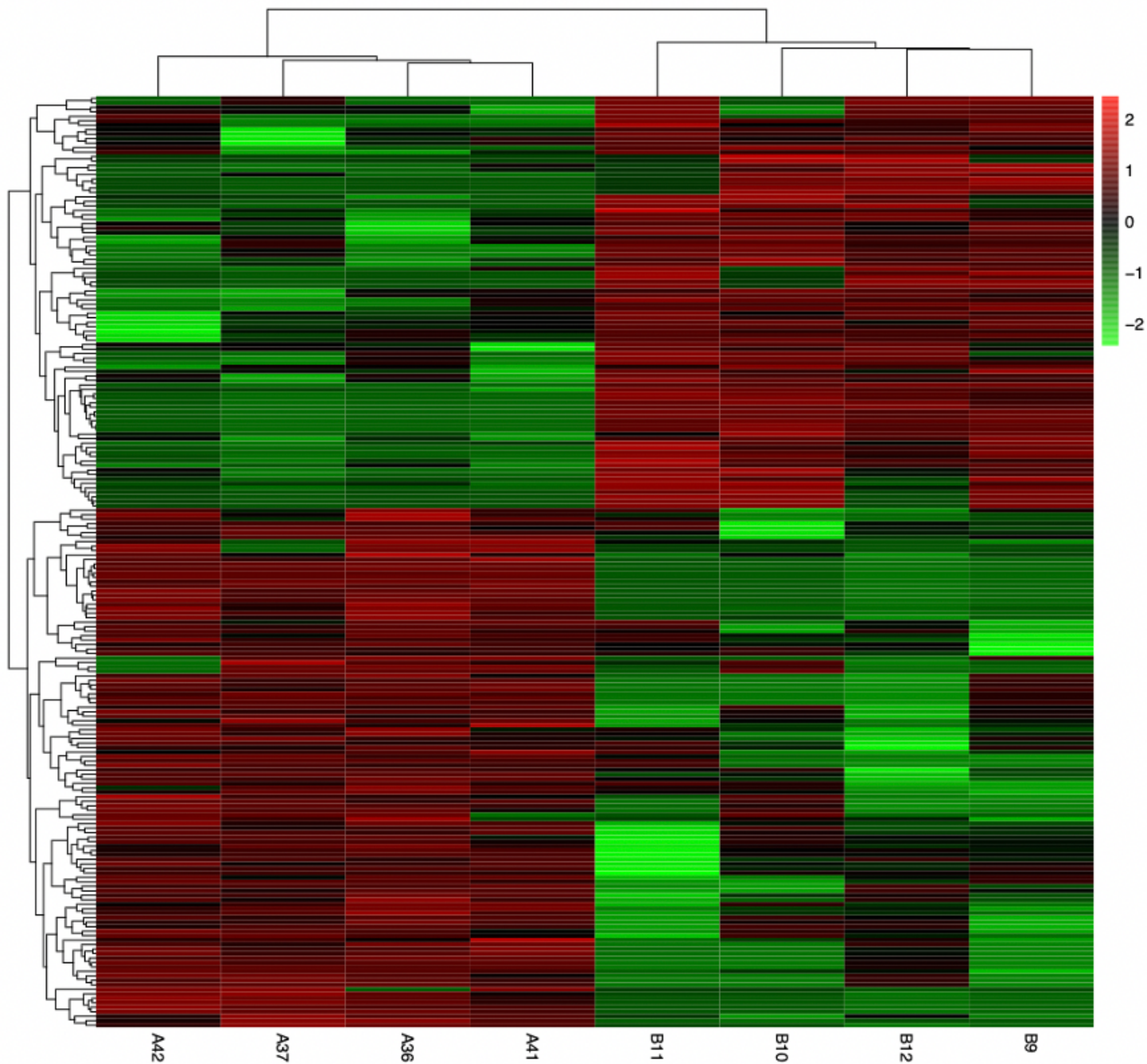


**Figure 2**

Clustering results of differentially expressed circRNAs. Each column denotes a sample and each row represents a dysregulation of RNA transcription. Red indicates upregulated genes, green indicates downregulated genes.

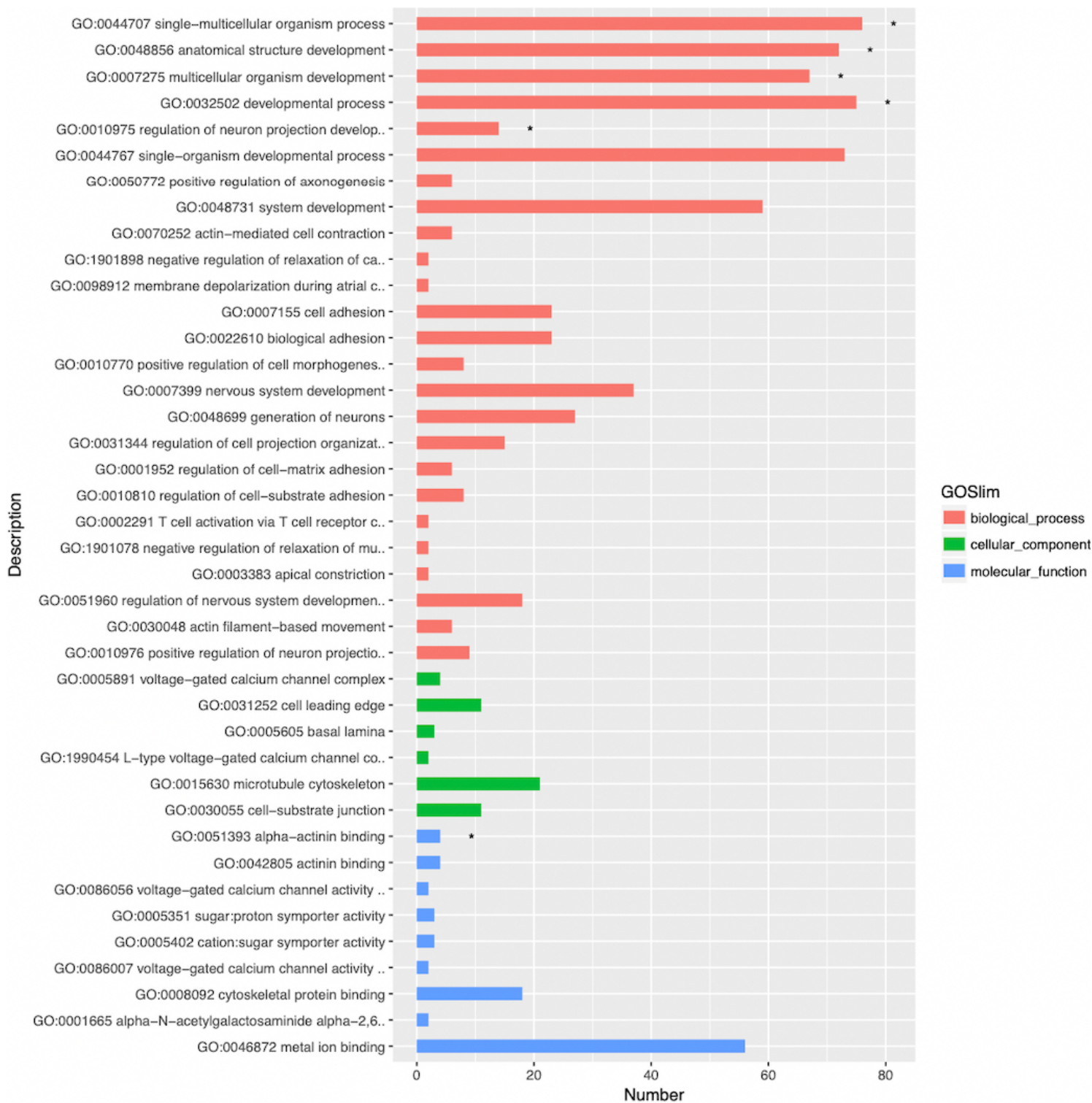


**Figure 3**

GO enrichment analysis of differentially expressed genes between the two groups. Red indicates the enrichment number of circRNAs in BP, green represents the enrichment number of circRNAs in CC, and blue represents the enrichment number of circRNAs in MF. The column shows functional terms associated with the identified circRNAs. The abscissa represents circRNAs number in each functional term. GO, Gene Ontology; BP, the biological process; CC, cellular components; MF, the biological process; circRNA, circular RNA.

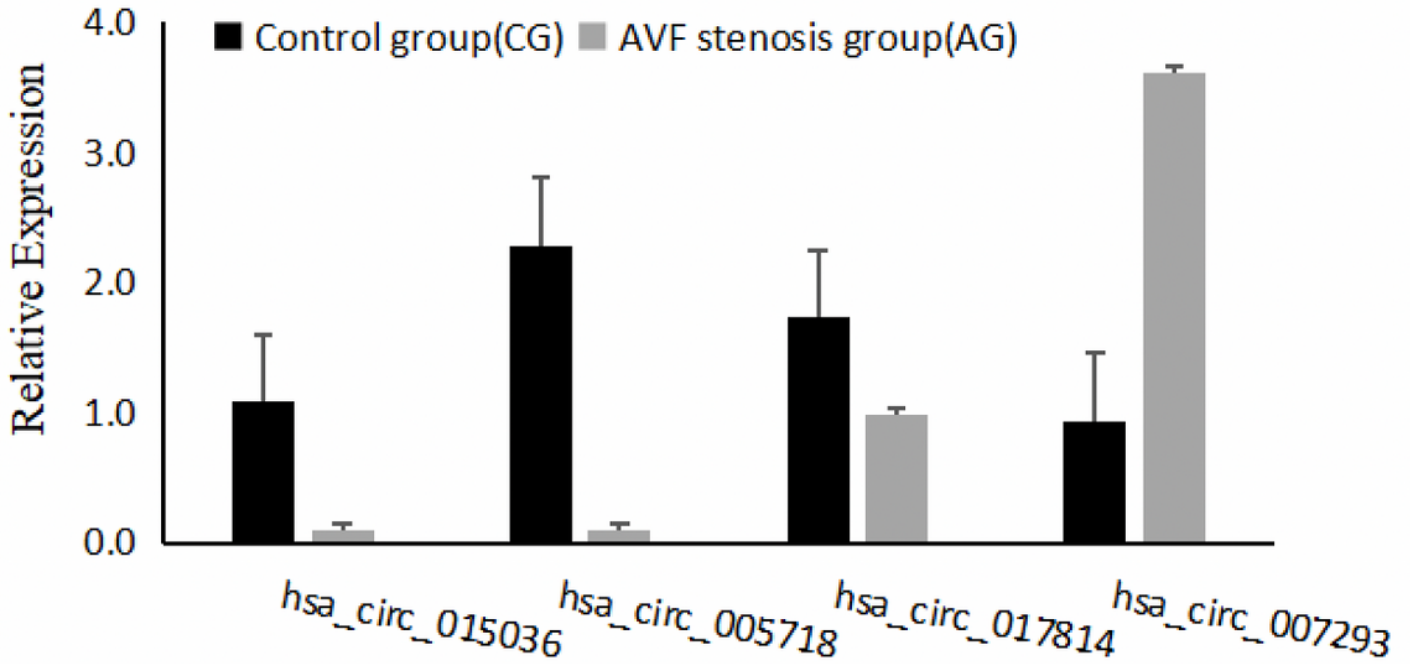
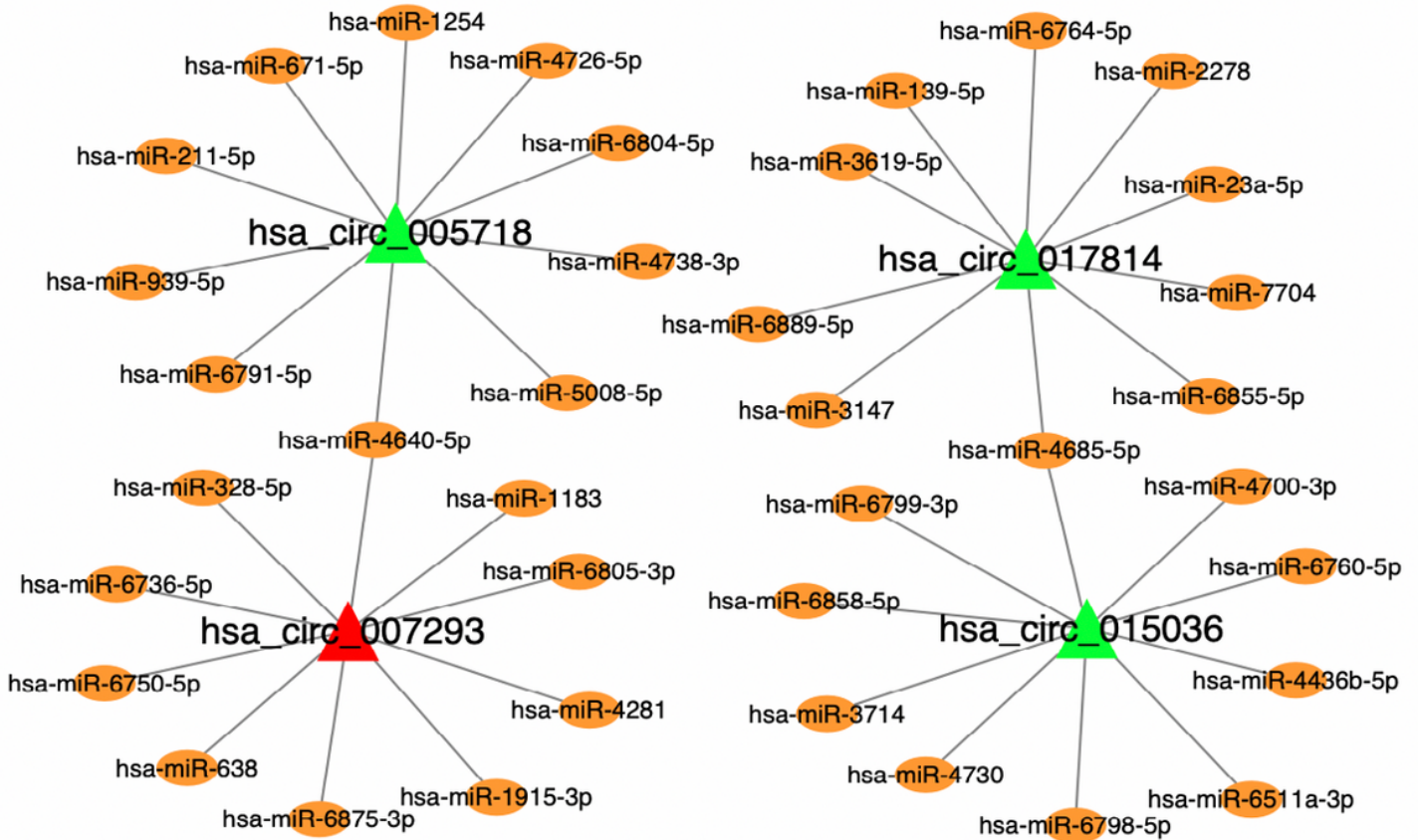


Figure 4

Validation of circular RNA expression levels via qRT-PCR analysis of AG and CG. The relative expression levels of four DE circRNAs are indicated as the ratio of average  $2^{-\Delta\Delta CT}$  (log2 transformed). Data is expressed as mean  $\pm$  SD, the statistical threshold considered is  $P < 0.05$ . AG: AVF stenosis group; CG: Control group. DE circRNAs: differentially expressed circRNAs; circRNA, circular RNA.



## Figure 5

The circRNA-miRNA interaction network. The four differentially expressed circRNAs (Green represents downregulated circRNAs, red represents upregulated circRNAs) are in the triangles, and their top 10 targeted miRNAs are in the yellow ellipses. circRNA, circular RNA; miRNA, microRNA.

## Supplementary Files

This is a list of supplementary files associated with this preprint. Click to download.

- [Supplementarymaterials.docx](#)